Online Supplemental Information.

1) Differences with Ball et al. (1999).
2) Variation of Mixing Region temperature
3) Measured [H_2SO_4] vs. Q_A
4) Long time monitoring of NBC
5) Differential Mobility Analyzer. Particle sizes.
6) More data sets for particle vs. MS ion ratio or Q_A.
7) Ammonia and amine additions.
8) Previous work on amines/ammonia
9) Contamination Episode.
10) Preliminary Fluid Dynamics results

1 Differences with Ball et al.

There are significant differences with the procedure of Ball et al. (1999) and it is assumed that these differences have little effect on the results. They are listed here for completeness. As noted in the text, Q_A, the N_2 flow rate over the sulfuric acid reservoir was varied to attain variations in H_2SO_4 content: also, the small tube carrying this flow was ~ 29 °C whereas in Ball et al. it was maintained at 60 °C.

There was also (i) a higher pressure, 1 atm vs. 0.8 atm, and (ii) a larger mass flow rate, 6 sLpm vs. 5 sLpm. The overall effects of (i) and (ii) result in an average flow velocity that is similar to that of Ball et al. Buoyancy driven convection is expected to be similar.

There was no (iii) periodic rinsing of the flow reactor with de-ionized water as was done by Ball et al. Rinsing the flow reactor was not done because it would be exposed to room air which is not desirable. The reproducibility of the results supports this decision. However, at one point the dry N_2 flow line (Teflon) was T-ed into to introduce an amine to this flow (and thus the mixing region); upon withdrawing the amine, particle count rates subsided quickly but plateaued after a few days at ~300 s^{-1} for NBC, indicating the line became contaminated with the amine (normal NBC conditions yield particle count rates of ~ 20 s^{-1}.) This line was removed from the system, rinsed with a 10^{-3} M HCl solution and then deionized water, dried and replaced whereupon NBC conditions yielded a typical particle count rate of 15 s^{-1}.

The chemical ionization mass spectrometer (iv) had an ion drift region - Hanson (2005), ion molecule reaction times of ~ 1 ms set by electric fields - rather than a flow arrangement - Eisele and Tanner (1993), ion molecule reaction times of ~1 s set by gas flows - and (v) ammonia was introduced below the mixing region rather than in it. The drift arrangement (iv) is less sensitive than the flow arrangement but [H_2SO_4] is more readily calculated in the absence of calibrations. Nonetheless, both systems are passive monitors of sulfuric acid and should yield equivalent results. The differences in ammonia introduction methods means that a direct comparison between the ammonia addition experiments should be made with caution.

The nucleation time (vi) here of 8 s is different than that used by Ball et al. of 4 s which was based on a 4 cm/s flow velocity over the ~ 15 cm nucleation zone length. A more refined estimate here was obtained by using their Figure 3(a) data and noting that a 4 cm/s speed applies to 1/3 of this length, 2.5 cm/s applies to the middle third, and 1 cm/s applies to the top portion. The sum of times in these portions of the nucleation zone is about 8 s, which is assigned a large uncertainty of +100%, -50%. Further exploration of the time for nucleation in a flow reactor will be done with fluid dynamics simulations.

Finally, the particle inlet here did not extend into cooled section of the flow reactor which is believed to lead to a high variability in the present measurements.

2 Variation of mixing region temperature.

Temperature of the mixing region was varied over the range of 30 to 45 C and particle numbers decreased considerably as temperature increased. This is due to suppression of nucleation in the mixing region, and to a lesser extent, changes in flow patterns in the transition and nucleation regions. This is shown in Fig A1(a) for NBC and a set of data taken ~13 months earlier (b), a few weeks after the system was initially assembled and at a total flow rate of 4 sLpm. A much stronger dependence on mixing region temperature is exhibited in Fig. A1b. The stronger effect may be due to the lower flow rate and also to contaminants that may be present initially in the system. Further experimentation on this effect with N bases present in the mixing region are planned.

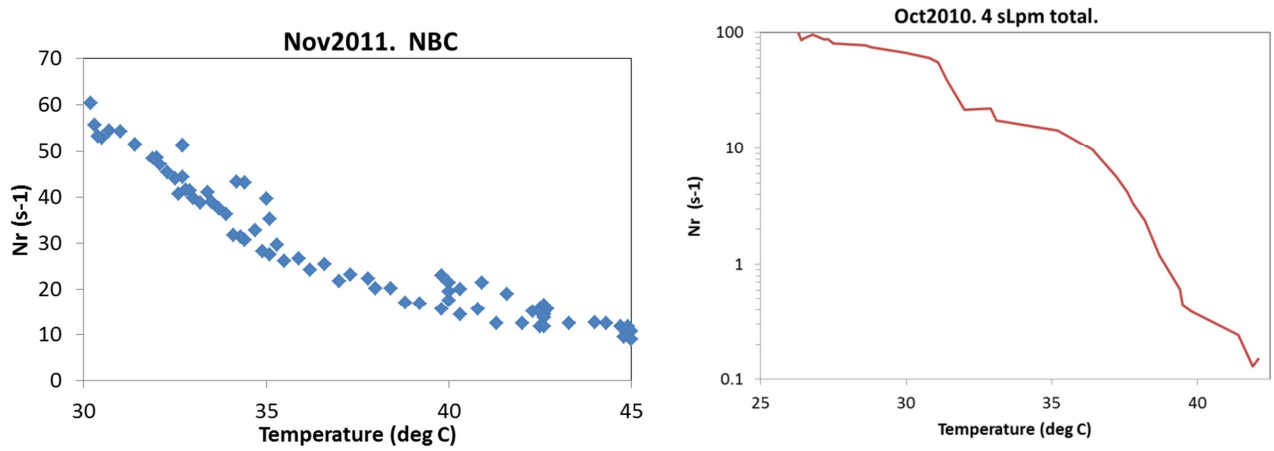

(a) (b)

Fig. A1. Variation of particle counts as a function of mixing region temperature. Results of the particle number versus mixing region temperature performed in (a) Nov 2011 and (b) Oct 2010.

3 Mass spectrometer detection vs QA, flow rate through sulfuric acid reservoir.

Shown in Fig. A2 (a) and (b) are the ion signals for sulfuric acid versus flow rate. A linear relationship is shown. Evident in Fig. A2b, deviations from this relationship occurs for flows higher than about 1.6 sLpm. This dropoff at high flow rates is due to (i) undersaturation due to finite diffusion and/or (ii) cooling of the H_2SO_4 reservoir by the nitrogen gas.

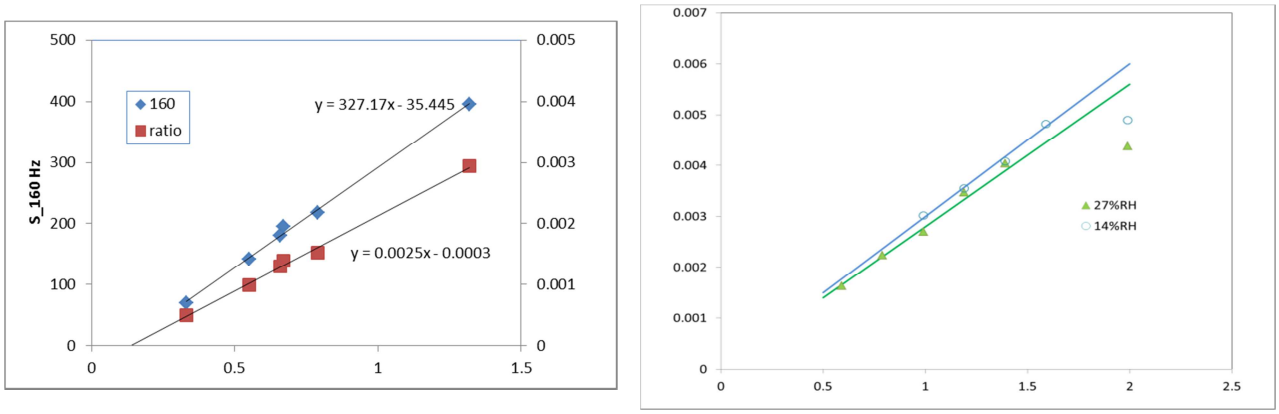

(a) (b)

Figure A2. (a) Variation with Q_A (sLpm) of the raw signal at 160 u ($HSO_4^- \cdot HNO_3$). (b) The ratio of signals for the HSO_4^- core ion and the NO_3^- core reactant ions plotted versus Q_A showing the non-linear relationship above 1.5 sLpm.

4 Nr for NBC conditions for 10 months.

A plot of measured count rates with time for NBC is shown in Figure A3. A general downwards trend is exhibited: an exponential decay plus a constant (i.e., $Ae^{-bt} + C$) is plotted as a suggested time dependency. A contamination episode is indicated during the months of May and June 2011 which is explained below. Note that the large spikes in early June are due to heating of contaminated lines that were then cleaned or replaced.

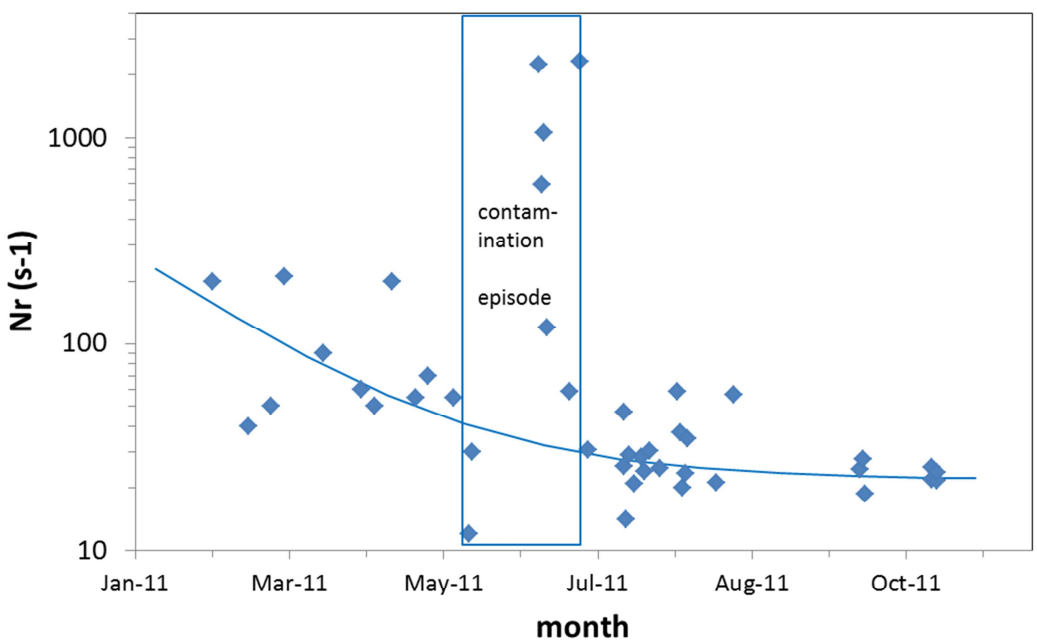

Figure A3. Nr versus date, for 10 mos. Beginning in late Jan-11, NBC conditions were chosen with total flow rate of 6 sLpm and T_{H2SO4} reservoir = 30 C.

5 Representative data sets for N_r vs. MS ion ratio and Q_A

A plot representative of the scatter of particle count rate vs. ion ratio from negative ion AmPMS is shown in Figure A4. This is all the data for the month of August, 2011. For most of June and July 2011, AmPMS was not operational and the nucleation data is plotted as N_r vs. Q_A (for $Q_A \leq$ 1.5 sLpm) in Figure A5: (a) 14 % RH and (b) 40% RH.

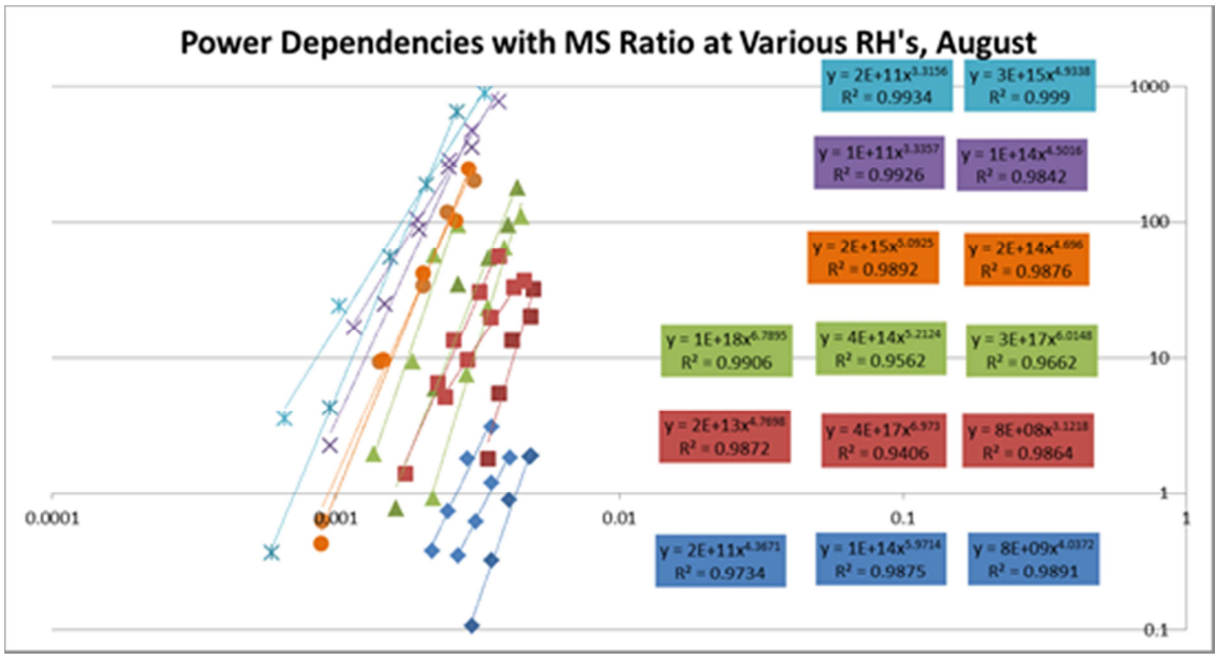

Figure A4. N_r plotted versus MS ion ratio for a range of relative humidities: solid blue diamonds, 14%; red squares, 20 %; green triangles, 27%; orange circles, 40%; purple X, 54%; turquoise *, 68 %.

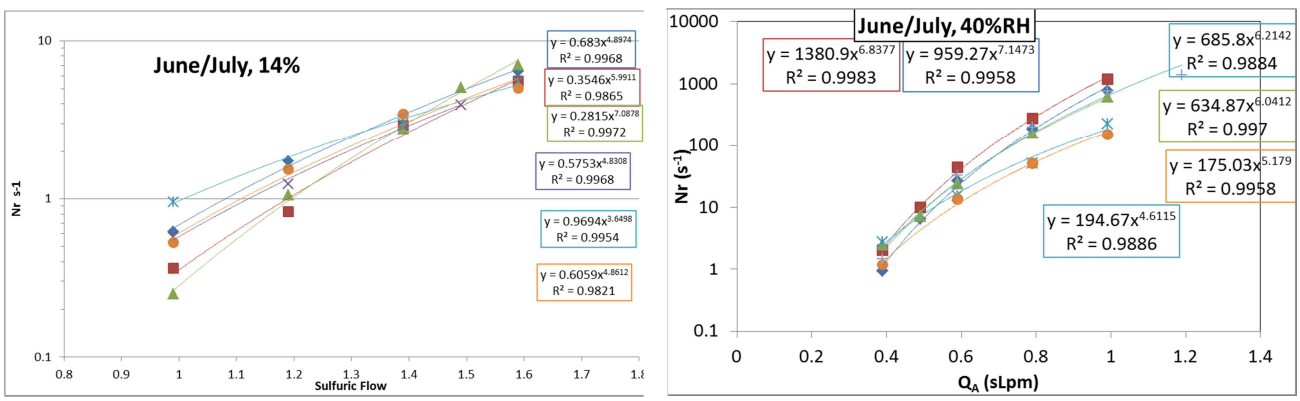

(a) (b)

Figure A5. N_r plotted versus Q_A at (a) 14 % rh and (b) 40% RH.

6 Particle Sizes.

The particle size distributions for Q_A= 1 and 0.4 sLpm are shown in Figure A6. These two sets of conditions represent typical and low sulfuric acid concentrations respectively. Particle charging efficiency of Fuchs [1964] and long DMA loss equation of Birmili et al. [1997] were applied. The log normal particle distributions are shown and have peak diameters of 6 and 7.7 nm and lnσ was 0.25-to-0.3. Even though the charging of nanoparticles by the custom-built

charger has not been evaluated and the particle sampling lines may cause additional particle losses, this measurement shows that the particle sizes are well above the detection threshold of the instrument, about 2 nm in diameter.

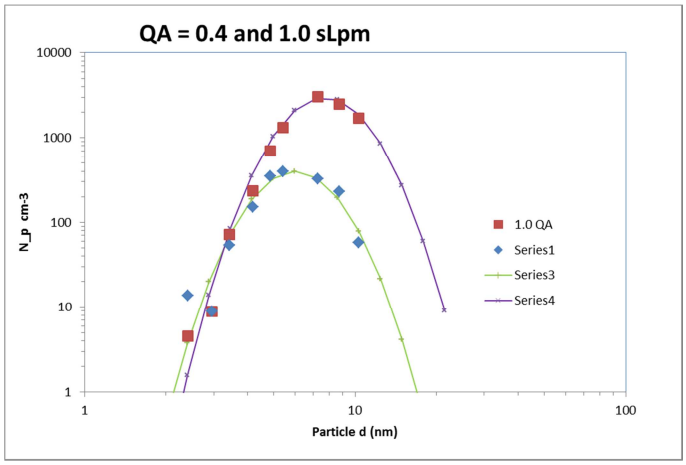

Figure A6. Particle size distributions for two different sulfuric acid levels. A rough conversion of the vertical axis, Nr, to dN/dlnD can be done by multiplying by the ratio of sheath to aerosol flows [Stolzenburg and McMurry, 2008] (sheath flow was 7.2 sLpm and the aerosol flow was 1.3 sLpm.)

As discussed in the text, Kuang et al. (2012) presented modified conditions for UCPCs where the saturator temperature of the UCPC is increased, thereby increasing the detection efficiency of nanoparticles of 2 nm diameter and smaller. To test if the particles detected here are of this size, different saturator temperatures were used for experiments at NBC. It was found that when the saturator temperature was increased (and condenser flow was increased), the particle number density did not change, however the pulse heights (i.e., channel number from the multichannel analyzer, Maestro, EG&G Optics) decreased. The pulse heights correspond to the size of the particles after growth with butanol which is in accordance with the Kuang et al. modification. The important result is that the modified conditions did not affect N_p, the detected number density of nanoparticles. This observation indicates that the nanoparticles formed in the experiment are likely to be of a significantly greater size than ~2 nm diameter.

7 Ammonia and amine additions.

7.1 Upper Limits to Amines

Shown in Figure A7 is a 5 Hr time period of AmPMS data where the flow reactor effluent was sampled with AmPMS with the zeroing mechanism deployed. Plotted versus time are the gross

mixing ratios (pptv) for the C1, C2, C3, and C4 amines (e.g., methyl-, dimethyl-, trimethyl-, diethyl-, or isomers.) Three zeroes, each about 10 min long, are indicated. The upper limits to the mixing ratios for methyl- and dimethyl- amine are 0.3 and 1 pptv, respectively. The C3-amine (60 u) appears to have an initial 1-2 pptv uptick upon zeroing but decreases to background in ~10 min. This could be due to a possible contamination in the three way valve connecting the inlet line, the zeroing line, and the instrument. The three way valve had not been cleaned after the system had been exposed to outdoor air for several weeks.

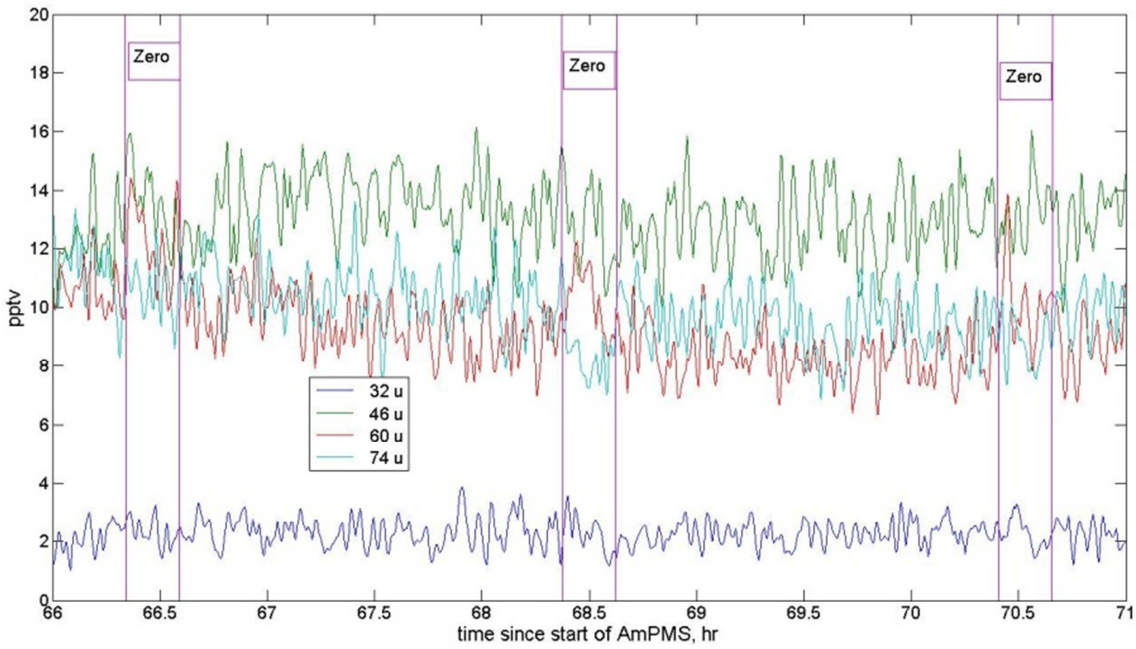

Fig. A7. Signals for AmPMS converted to mixing ratio (pptv) for four alkyl amines. AmPMS was connected to the bottom of the flow reactor with a zeroing mechanism. Three zeroing stages are shown.

7.2 Effect of 10 ppqv of base.

A decrease in the vapor pressure of H_2SO_4 due to base would increase the stability of H_2SO_4 in the critical cluster. This can be estimated using the E-AIM website (Clegg et al., 1998.) At 30 % RH and a 0.3-to-1 NH_4^+ to sulfate ratio (suppressing formation of ammonium bisulfate) the equivalent NH_3 and H_2SO_4 mixing ratios at 1 atm total pressure are about 10 and 7 ppqv, respectively. Because this is close to that for H_2SO_4 vapor over neat H_2SO_4-H_2O solution at 30 % RH (9.7 ppqv), this level of ammonia would probably not significantly affect nucleation. With methyl amine (Ge et al. 2011b) in the H_2SO_4-H_2O calculations, a one to one mole ratio of methyl amine to sulfuric acid at 30 % RH gives equivalent mixing ratios (1 atm total pressure) of

2.4 ppqv for H_2SO_4 and ~10 ppqv for methyl amine. Note: in the current implementation there are important assumptions regarding the amine's activity coefficients in sulfuric acid solutions (S. Clegg, 2011, private communication.) Nonetheless, the suppression of the partial pressure of H_2SO_4 due to base is likely to be less in small clusters than for bulk solutions, and therefore only a modest effect on particle formation is expected due to the presence of 10 ppqv levels of NH_3 while a significant effect for methyl amine at 10 ppqv levels cannot be ruled out.

7.3 Base addition considerations.

The ~30 pptv level of amine added at the top port resulted in extremely high N_r for $Q_A = 1$ such that live time was reduced to essentially 0 and thus N_p could not be reliably monitored. For the base addition experiments therefore, Q_A was set to 0.4 sLpm for 27 % RH measurements: this being the lowest sulfuric acid level used in any neat experiment (i.e., for experiments from 40 % to 68 % RH.)

Different addition methods (for example, 1.7 mm ID vs. 4 mm ID inlet tubes) resulted in significantly different N_r for nominally the same amine mixing ratios. The variability here was most likely due to how well the base was mixed into the main flow: a smaller ID tube has a stronger jet, which can go across the flow reactor and interact rapidly with the wall. This was verified in an experiment where a constant amount of methyl amine was introduced at the bottom of the flow reactor (see bottom port in Fig. 1) with varying amounts of N_2 flow through the inlet. The AmPMS "measured" amine concentration varied from 3 to 17 pptv with varying inlet tube flow rates of 10 to 150 STP cm^3/min; above ~40 STP cm^3/min [amine] decreased strongly. The maximum observed level of ~17 pptv is consistent with the calculated amount added, 25 pptv. Amine and ammonia addition are discussed in Panta et al. (2012) and calibrations will be presented in Carlson et al. (2012).

8 Previous work on amines/ammonia.

Enhancement factors (EF) for ammonia and amines are convenient for quantifying and reporting their effects on nucleation. It is defined as the ratio of particles formed in the presence of added base to that in the absence of added base.

For NH_3 for example, Kirkby et al. (2011) report EF of ~100 for 70 pptv NH_3 (6 pptv H_2SO_4 and 38 % RH); Ball et al. (1999) show an EF of ~20 for an estimated NH_3 of ~3 pptv (+200/-67 %) at

15 % RH and ~1000 pptv H_2SO_4; Berndt et al. (2010) report EFs up to 100 for 50 ppbv (nmol mol^{-1}) at low RH but less than 10 at 47 % RH. Benson (2010, 2011) report EF of 10 or less for 20 ppbv for RH values of 15 % and higher. Yu et al. (2012) report EFs for addition of ammonia and methyl amine at the single digit ppbv level of ~10-to-200. These values are much lower than the ~ 10^3 to 10^5 values reported here for 3 to 45 pptv, respectively, for ~ 200 pptv $[H_2SO_4]_{NZ}$. The differences of the present results with Ball et al. can be explained because of differing H_2SO_4 levels; at lower H_2SO_4, the EF due to NH_3 will increase according to theory (Coffman and Hegg, 1995). The studies with very large N-base levels that have low EFs also generally have low amounts of H_2SO_4. Also, low EFs can be due to the presence of contaminants: as discussed in the text, and by Kirkby et al. (2011), Benson et al. (2011), and Yu et al. (2012).

Comparisons of the present measurements to the predictions for ammonia's effect on nucleation seem to indicate that the predictions either overestimate nucleation rates or EFs. The Coffman and Hegg (1995) predictions show EFs of ~100 and 1000 for 1 and 5 pptv respectively (for 75 % RH and 200 pptv H_2SO_4) however nucleation rates are predicted to be ~10^{10} to 10^{15} cm^{-3} s^{-1}. Korhonen et al. (1999) suggest an EF of ~ 10^{14} at 2 pptv (52 % RH and 10^9 H_2SO_4) and J = 10^5 cm^{-3} s^{-1} and Napari et al. (2002) an EF of 10^8 for 2 pptv (using 0.1 pptv as the binary nucleation rate) with J = 10^4 cm^{-3} s^{-1}. The enhancement factor reported here is in better agreement with the theoretical treatment of Coffman and Hegg (1995) however the measured nucleation rate of 5 cm^{-3} s^{-1} is very much lower (a factor of 10^9 or greater) than they predict. Although the EF of Korhonen et al. and Napari et al. deviate significantly from the current measurement, their predicted rates are somewhat closer, factors of only 10^3-10^4 too large.

9 Contamination Episode.

For a period of time there was an unknown contaminant in the system, evidenced by a sharp rise in particle numbers, to almost uncountable levels for periods of tens of minutes during heating of suspected contaminated lines. To investigate further the effect this contaminant had on the experiment, several power dependencies were taken at 27% RH while particle numbers remained above normal NBC. They decreased day after day as the contaminant was slowly eliminated from the system, and normal levels for NBC were achieved in about a ten days. While particle numbers were high and as they decreased, the power dependency did not vary (Figure A8). It is concluded that the unknown contaminant "X" changed only the total number of particles, not the

power dependency on H_2SO_4, and by extension the number of H_2SO_4 in the critical cluster. The mass spectrometer system was not operational for most of this episode.

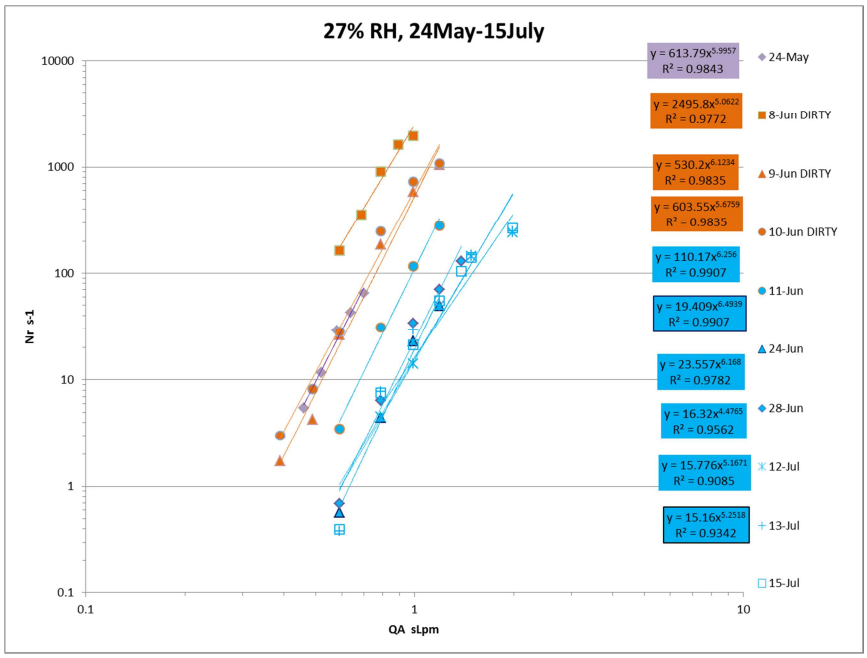

Figure A8. N_r and power dependencies at 27% RH during contamination episode. Data for May 24th, June 8th to 11th all show enhanced particle numbers but power dependencies were not appreciably affected.

10 Computational Fluid Dynamics: $[H_2SO_4]_{NZ}$ versus measured $[H_2SO_4]$.

Shown in Figures A9 and A10 are contour plots of the mass fraction of H_2SO_4 in a 2D simulation of the flow reactor. The diffusion coefficient for H_2SO_4 in N_2 was taken from Hanson and Eisele (2000). Thermal properties of the gas mixtures are very close to those used by Herrman et al. (2010). A complete description of the model is under review (Panta et al., [2012]).

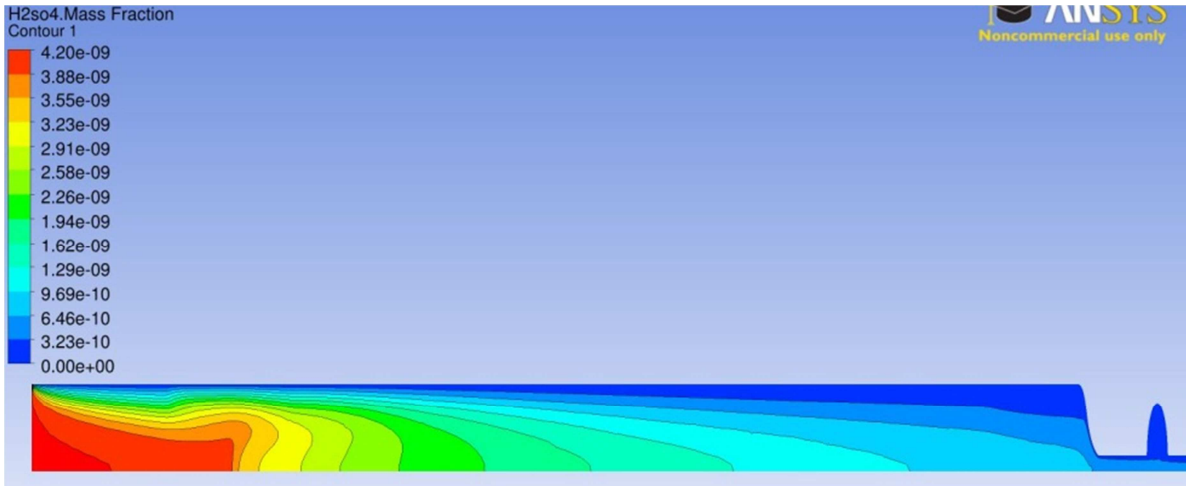

Figure A9. Mass fraction contours of H_2SO_4. Axis of symmetry is at the bottom, vertical coordinate is multiplied by ten. Nucleation zone is about 1/3 down the tube with an average mass fraction of $2x10^{-9}$ for H_2SO_4.

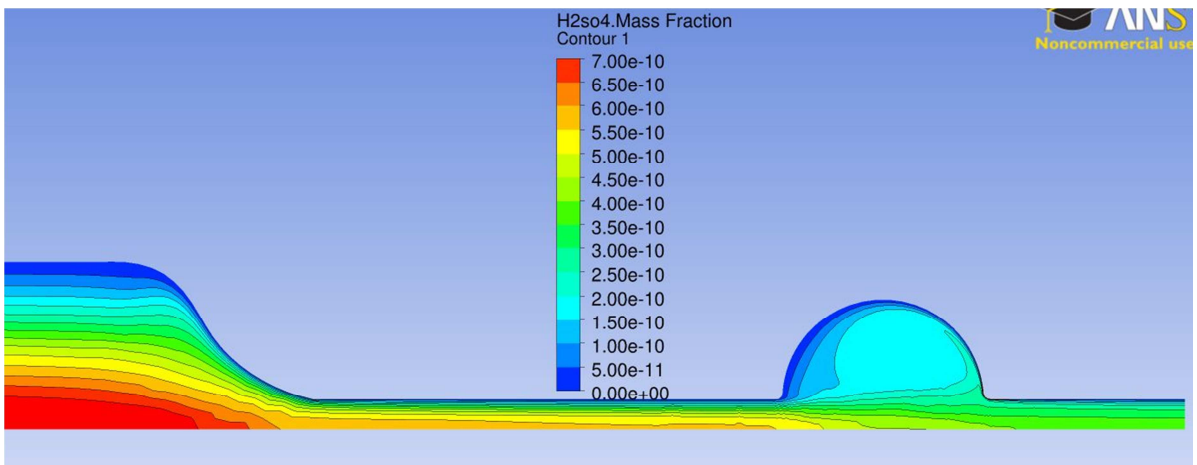

Figure A10. Blowup of mass spectrometer detection region in the middle of the small sphere of radius 1.5 cm. Average H_2SO_4 mass fraction is about $3x10^{-10}$ in the ion drift region.

References

Clegg, S. L., Brimblecombe, P., A. S. Wexler (1998) A thermodynamic model of the system H^+-NH_4^+-SO_4^{2-}-NO_3^--H_2O at tropospheric temperatures. J. Phys. Chem. A 102, 2137-2154. (http://www.aim.env.uea.ac.uk/aim/aim.php)

Eisele, F.L., and Tanner, D. J.: Measurement of the gas phase concentration of H2SO4 and methane sulfonic acid and estimates of H2SO4 production and loss in the atmosphere, J. Geophys. Res., 98, 9001, 1993.

Ge, X., Wexler, A. S., Clegg, S. L. (2011b) Atmospheric amines - Part II. Thermodynamic properties and gas/particle partitioning. Atmos. Environ. 45, 561-577.

Korhonen, P., M. Kulmala, A. Laaksonen, Y. Viisanen, R. McGraw, and J. H. Seinfeld, Ternary nucleation of H_2SO_4, NH_3 and H_2O in the atmosphere, J. Geophys. Res., 104, 26,349–26,353, 1999.

Napari, I., M. Noppel, H. Vehkama¨ki, and M. Kulmala (2002), Parametrization of ternary nucleation rates for H_2SO_4-NH_3-H_2O vapors, J. Geophys. Res., 107(D19), 4381, doi:10.1029/2002JD002132.

Stolzenburg, M.R., P. H. McMurry, Equations Governing Single and Tandem DMA Configurations and a New Lognormal Approximation to the Transfer Function, Aerosol Science and Technology, 42:421–432, 2008.